

Synthesis and Characterisation of New Nickel-Iron Complexes with an S₄ Coordination Environment around the Nickel Centre

Johanna A. W. Verhagen,^[a] Martin Lutz,^[b] Anthony L. Spek,^[b] and Elisabeth Bouwman*^[a]

Keywords: Nickel / Iron / S ligands / Electronic structure / Electrochemistry

The nickel complex [Ni(xbsms)] [H₂xbsms is *α,α'*-bis(4-mercapto-3,3-dimethyl-2-thiabutyl)-*o*-xylene] was reacted with FeCl₂, [Fe₂(CO)₉], [Fe(CO)₂(NO)₂] and [Fe(CO)₄I₂]. The reaction with FeCl₂ gives the heterotetranuclear nickel–iron complex [Ni(xbsms)FeCl₂]₂. The complex was characterised by analytical, spectroscopic and electrochemical methods and by X-ray diffraction. [Ni(xbsms)FeCl₂]₂ crystallises in the monoclinic space group *P*2₁/*c*, with the dimer located on the inversion centre. The nickel ions are in a square-planar S₂S'₂ environment, comprised of two thioether and two thiolate sulfur atoms. The thiolate sulfur atoms form a bridge between the nickel ion and the iron centre. The iron ions are in a pseudo square-pyramidal S₂Cl₃ environment, with two chloride ions forming a bridge between the two iron centres.

The Ni–Fe distance is 3.0403(3) Å. The reaction with [Fe₂(CO)₉], [Fe(CO)₂(NO)₂] or [Fe(CO)₄I₂] gives the heterodinuclear complexes [Ni(xbsms)Fe(CO)₄], [Ni(xbsms)Fe(NO)₂] and [Ni(xbsms)Fe(CO)₂I₂], respectively. These complexes were characterised by analytical, spectroscopic and electrochemical methods. In [Ni(xbsms)Fe(CO)₄], one thiolate group bridges the Ni and Fe centres, whereas in [Ni(xbsms)Fe(NO)₂] and [Ni(xbsms)Fe(CO)₂I₂], two thiolate groups form a bridge between the centres. These newly synthesised nickel–iron complexes appear to be suitable complexes for new structural models for [NiFe]-hydrogenases.

(© Wiley-VCH Verlag GmbH & Co. KGaA, 69451 Weinheim, Germany, 2003)

Introduction

Hydrogenases are widespread among several classes of anaerobic and occasionally aerobic bacteria, and were first discovered in the 1930s.^[1] These enzymes catalyse the reversible oxidation of dihydrogen, which allows the cell to generate or dispose of reducing equivalents during respiration. In vitro hydrogenases also catalyse H⁺/D₂ exchange.^[2] The reactivity of nickel enzymes in the generation or consumption of dihydrogen is interesting because of the fact that possible future energy problems may be solved using a hydrogen economy.^[3] By studying the synthesis and characterisation of structural and functional models for the hydrogenases, we hope to contribute to the development of catalysts for, for example, fuel cells.

The hydrogenases have been divided into two main classes, based on their metal content, namely [NiFe]-hydrogenases and [Fe]-hydrogenases.^[2] A subset of the first class has been shown to contain selenium, the [NiFeSe]-hydrogenases. Furthermore, a hydrogenase that does not contain any transition metal has been discovered.^[4] Extensive stud-

ies and characterisations, including single-crystal X-ray diffraction, have revealed the structure of several [NiFe]-hydrogenases.^[5,6] The X-ray studies have shown that the active sites of the [NiFe] enzymes isolated from *Desulfovibrio gigas*^[5] and *Desulfovibrio vulgaris*^[6] contain the heterodinuclear site [(Cys-S)₂Ni^{II}(μ-S-Cys)₂Fe^{II}(CN)₂(CO)], in which the nickel centre has an S₄ coordination environment. Two thiolate sulfur atoms form a bridge between the nickel and the iron centres. Furthermore, three diatomic molecules are coordinated to the iron centre, two CN molecules and one CO molecule. In the last few years, considerable interest has been shown in the structural modelling of the [NiFe]-hydrogenases.^[7–12] However, most of the structural models have a mixed-donor environment around the nickel centres. A variety of square-planar nickel complexes have been synthesised with only sulfur donor atoms in the coordination environment,^[13] and several nickel–iron complexes relevant for hydrogenase modelling have been synthesised.^[2,14–18] However, so far only one heterodimetallic nickel–iron complex that has an S₄ coordination environment around the nickel centre has been reported.^[19] In this paper, we describe the synthesis of new heterometallic nickel–iron complexes, starting from a nickel complex with an S₄ coordination environment.^[20]

Results and Discussion

Syntheses: Four new nickel–iron complexes were synthesised by the reactions of [Ni(xbsms)] with the iron com-

^[a] Leiden Institute of Chemistry, Gorlaeus Laboratories, Leiden University, P. O. Box 9502, 2300 RA Leiden, The Netherlands
Fax: (internat.) + 31-71/527-4451
E-mail: bouwman@chem.leidenuniv.nl

^[b] Bijvoet Center for Biomolecular Research, Crystal and Structural Chemistry, Utrecht University, Padualaan 8, 3584 CH Utrecht, The Netherlands

plexes FeCl₂, [Fe₂(CO)₉], [Fe(CO)₂(NO)₂] and [Fe(CO)₄I₂]. The ligand H₂xbmsms, *a,a'*-bis(4-mercapto-3,3-dimethyl-2-thiabutyl)-*o*-xylene, is a tetradentate ligand, which coordinates to the nickel centre through two thiolate groups that are forced in the *cis* positions. These thiolate groups provide a potential binding site for an iron centre.

The reaction of [Ni(xbmsms)] with FeCl₂ produces the complex [Ni(xbmsms)FeCl₂]₂ (**1**). In this synthesis either anhydrous FeCl₂ or FeCl₂·4H₂O can be used. Single crystals suitable for X-ray diffraction were obtained from the filtrate on standing at room temperature, after the removal of the initially formed precipitate.

The reaction of [Ni(xbmsms)] with half an equivalent of [Fe₂(CO)₉] gives the complex [Ni(xbmsms)Fe(CO)₄] (**2**), and that with [Fe(CO)₂(NO)₂] the complex [Ni(xbmsms)Fe(NO)₂] (**3**).

The synthesis of [Ni(xbmsms)Fe(CO)₂I₂] (**4**) was performed in chloroform and the reaction mixture was cooled to 273 K in the absence of light. These conditions are necessary for the two CO molecules to remain coordinated to the iron centre. If the synthesis of **4** is carried out in acetonitrile, a compound is formed that lacks CO signals in its IR spectrum. This compound might have a structure that is similar to that of **1**; however, the exact nature of this product is still unknown.

All the complexes are moderately soluble in polar solvents. Furthermore, all the complexes decompose very rapidly in air and in solution. Complex **1** is the most stable, followed by complex **4**, and thereafter complexes **2** and **3**. Decomposition of complexes **2** and **3** leads to the regeneration of the parent nickel complex. Decomposition of **4** begins with the loss of the CO groups. The instability of complexes **2**, **3** and **4** is reflected in their NMR spectroscopic and magnetic susceptibility data. These complexes are diamagnetic as is confirmed by ¹H NMR spectroscopy; however, the μ_{eff} values are higher than expected as a result of decomposition to the paramagnetic species. The regenerated parent nickel complex can also be seen in the NMR spectra.

Structure of [Ni(xbmsms)FeCl₂]₂ (1**):** A projection of the structure of the complex [Ni(xbmsms)FeCl₂]₂ is shown in Figure 1. Crystal data are given in Table 1 and selected bond lengths and angles are given in Table 2.

[Ni(xbmsms)FeCl₂]₂ crystallises in the space group *P*2₁/*c* with two molecules in the unit cell. The complex is heterotetranuclear with two Ni^{II} centres in a square-planar S₂S'₂ environment and two Fe^{II} centres in a pseudo square-pyramidal S₂Cl₃ environment. The molecule is located around an inversion centre. The two thiolate groups of the ligand xbmsms are forced in the *cis* positions, and form a bridge between one nickel and one iron centre. Furthermore, two thioether sulfur atoms are coordinated to the nickel centre. Two chloride ions form a bridge between the iron centres. The complex [(BME-DACO)NiFeCl₂]₂, reported by Darensbourg et al., has a similar hetero-tetranuclear structure, although, the nickel centre has an S₂N₂ coordination environment.^[11]

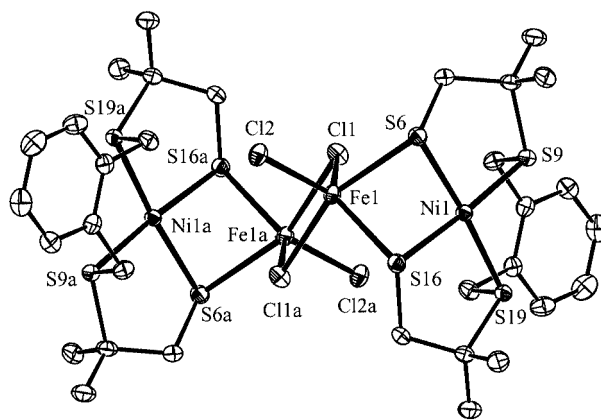


Figure 1. Displacement ellipsoid plot of [Ni(xbmsms)FeCl₂]₂, drawn at the 50% probability level. Hydrogen atoms are omitted for clarity. Symmetry operation a: 1 - x, -y, 1 - z

Table 1. Crystal and structure refinement data for the complex [Ni(xbmsms)FeCl₂]₂

Empirical formula	C ₃₂ H ₄₈ Cl ₄ Fe ₂ Ni ₂ S ₈
Molecular mass	1060.10
Crystal dimensions [mm]	0.06 × 0.20 × 0.20
Crystal system	Monoclinic
Space group	<i>P</i> 2 ₁ / <i>c</i> (no. 14)
<i>a</i> (Å)	11.5980(1)
<i>b</i> (Å)	10.2036(1)
<i>c</i> (Å)	18.5642(2)
β [°]	104.4206(4)
<i>V</i> (Å ³)	2127.70(4)
<i>Z</i>	2
<i>D</i> _{calcd.} [Mg·m ⁻³]	1.655
Absorption coefficient μ [mm ⁻¹]	2.208
No. of measured reflections	30020
No. of independent reflections	4830
No. of observed reflections [<i>I</i> > 2σ(<i>I</i>)]	4235
<i>R</i> 1 [^a] [obsd. refl./all refl.]	0.0218/0.0283
<i>wR</i> 2 [^b] [obsd. refl./all refl.]	0.0511/ 0.0535
<i>S</i> [^c]	1.038
No. of refined parameters	265

[^a] $R1 = \frac{\sum(|F_o| - |F_c|)}{\sum|F_o|}$. [^b] $wR2 = \frac{\{\sum[w(F_o^2 - F_c^2)^2] / \sum[w(F_o^2)^2]\}^{1/2}}$. [^c] $S = \frac{\{\sum[w(F_o^2 - F_c^2)^2] / (n - p)\}^{1/2}}$.

The coordination environment around the nickel ion has a small tetrahedral distortion, with an interplanar angle of 5.75(2)° between the planes S(6)–Ni(1)–S(9) and S(16)–Ni(1)–S(19).

The pseudo square-pyramidal environment of the iron centre is defined by the two thiolate sulfur atoms and two bridging chloride ions in the basal plane, and the terminal chloride ion Cl(2) in the apical position. The distortion towards a trigonal bipyramidal geometry is shown by S(6) and Cl(1a) in the apical positions and S(16), Cl(1) and Cl(2) in the trigonal plane. The two largest angles around the iron centre give a τ value of 0.45 (with τ = 0 for square-pyramidal and τ = 1 for trigonal bipyramidal geometries).^[21] The distance between the two symmetry-related iron centres is 3.6947(5) Å, indicating that no metal-metal interaction is present. From the geometry around the iron centre, it can be concluded that the iron centre is in a high spin state. This

Table 2. Selected bond lengths (Å) and angles (°) in $[\text{Ni}(\text{xbsms})\text{FeCl}_2]_2$ (symmetry position a: $1-x, -y, 1-z$)

Ni(1)–S(6)	2.1781(4)	S(6)–Ni(1)–S(9)	92.01(16)	Cl(1)–Fe(1)–Cl(2)	112.144(17)
Ni(1)–S(9)	2.2016(4)	S(6)–Ni(1)–S(16)	85.040(17)	Cl(1)–Fe(1)–S(6)	94.950(15)
Ni(1)–S(16)	2.1776(4)	S(6)–Ni(1)–S(19)	174.675(18)	Cl(1)–Fe(1)–S(16)	130.767(17)
Ni(1)–S(19)	2.1958(4)	S(9)–Ni(1)–S(16)	175.287(18)	Cl(1)–Fe(1)–Cl(1a)	82.726(15)
Fe(1)–S(6)	2.5197(5)	S(9)–Ni(1)–S(19)	91.104(16)	Cl(2)–Fe(1)–S(6)	100.386(16)
Fe(1)–S(16)	2.4462(5)	S(16)–Ni(1)–S(19)	91.566(16)	Cl(2)–Fe(1)–S(16)	116.896(17)
Fe(1)–Cl(1)	2.3927(4)			Cl(2)–Fe(1)–Cl(1a)	100.914(17)
Fe(1)–Cl(2)	2.2657(5)	Ni(1)–S(6)–Fe(1)	80.301(14)	S(6)–Fe(1)–S(16)	72.695(14)
Fe(1)–Cl(1a)	2.5286(5)	Ni(1)–S(16)–Fe(1)	82.005(15)	S(6)–Fe(1)–Cl(1a)	157.808(17)
		Fe(1)–Cl(1)–Fe(1a)	97.273(15)	S(16)–Fe(1)–Cl(1a)	92.062(15)

observation has been confirmed by the room temperature magnetic susceptibility measurements, which give a μ_{eff} value of $5.35 \mu_{\text{B}}$ per iron centre. This is consistent with a high spin Fe^{II} centre without any interaction between the two iron centres in the molecule.^[22]

The Fe–S–Ni angles of $80.301(14)$ and $82.005(15)^\circ$ lead to a Ni–Fe distance of $3.0403(3)$ Å. All distances and angles around the nickel centre are consistent with data of similar complexes in the literature.^[2,13]

Proposed Structure of $[\text{Ni}(\text{xbsms})\text{Fe}(\text{CO})_4]$ (2): A proposed structure based on elemental analysis and NMR spectroscopic studies is shown in Figure 2. This structure, containing a square-planar low spin Ni^{II} ion and a low spin $\text{Fe}(0)$ moiety, is similar to that of $[(\text{BME-DACO})\text{Ni-Fe}(\text{CO})_4]$.^[16] In the IR spectrum of complex (2), three signals assigned to the CO groups are observed at 2009, 1945 and 1860 cm^{-1} . These are slightly different from those reported for a THF solution of $[(\text{BME-DACO})\text{Ni-Fe}(\text{CO})_4]$,^[16] however, they are in the same region as the CO absorption observed at 1943 cm^{-1} for $[\text{NiFe}]$ -hydrogenase.^[23] The ^1H NMR spectrum shows resonance signals for every proton and every methyl group, which is in agreement with the proposed asymmetric structure. Using NOESY and COSY NMR spectra, full assignments of all resonance signals could be made. The ^1H NMR spectrum,

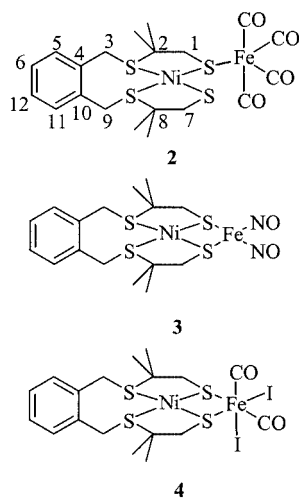


Figure 2. Schematic drawings of the postulated structure of $[\text{Ni}(\text{xbsms})\text{Fe}(\text{CO})_4]$ (2), $[\text{Ni}(\text{xbsms})\text{Fe}(\text{NO})_2]$ (3) and $[\text{Ni}(\text{xbsms})\text{Fe}(\text{CO})_2\text{I}_2]$ (4)

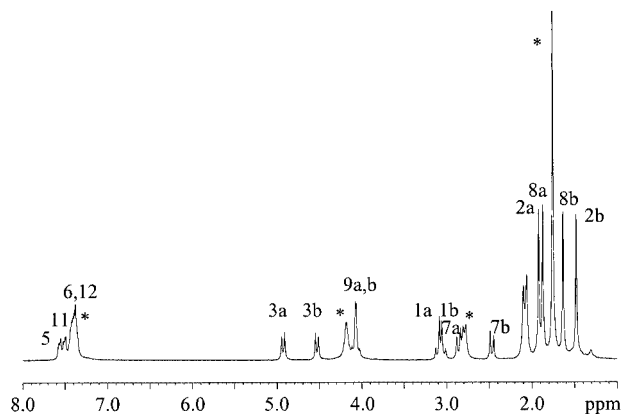


Figure 3. ^1H NMR spectrum of $[\text{Ni}(\text{xbsms})\text{Fe}(\text{CO})_4]$ in $[\text{D}_6]$ acetone at 253 K. Assignments in the figure correspond to numbers in Figure 2. The asterisks indicate signals from the decomposition product $[\text{Ni}(\text{xbsms})]$

recorded at 253 K, is shown in Figure 3. The parent nickel complex can also be seen in the NMR spectrum, as a result of the decomposition of the $[\text{NiFe}]$ complex. The ^{13}C NMR spectrum also reflects the asymmetry of the complex, all carbon atoms appear to be inequivalent. However, the CO resonance signals are not observed. This may be attributed to the low concentration and the instability of the complex, or to poor relaxation properties of the complex. The instability of the complex is confirmed by mass spectroscopy: $\{[\text{Ni}(\text{xbsms})\text{Fe}(\text{CO})_3] + \text{H}\}^+$ is observed as the main peak, indicating that one CO molecule is only loosely bound.

Proposed Structure of $[\text{Ni}(\text{xbsms})\text{Fe}(\text{NO})_2]$ (3): A proposed structure based on elemental analysis and ^1H NMR spectroscopy is also shown in Figure 2. This structure, containing a square-planar low spin Ni^{II} ion and a low spin $[\text{Fe}(\text{NO})_2]$ moiety, is similar to that of the Ni-Fe-nitrosyl complex reported by Osterloh et al.^[15] In the IR spectrum, strong signals assigned to the NO groups are clearly observed at 1771 and 1733 cm^{-1} . These absorptions are at significantly higher energies compared with those in the reported complex (1663 and 1624 cm^{-1}),^[15] and are also shifted relative to the starting Fe complex $[\text{Fe}(\text{CO})_2(\text{NO})_2]$ (1810 and 1766 cm^{-1}); however, they compare with those reported by Liaw et al. (1767 and 1725 cm^{-1}).^[17] The NO stretches in the IR spectrum are in the range reported for linearly coordinated NO^+ molecules.^[24] This indicates only a small increase in transfer of electron-density from Fe into

the π^* orbitals of the NO ligands, which is accompanied by the weakening of the NO triple bonds.

Proposed Structure of [Ni(xbsms)Fe(CO)₂I₂] (4): A proposed structure based on elemental analysis and mass spectrometry is also shown in Figure 2. The proposed structure is dinuclear with a square-planar low spin Ni^{II} ion, bridged via both thiolate sulfur atoms to the octahedral Fe^{II} ion. The IR spectrum of 4 is clearly different from that of 1, excluding a tetranuclear structure. Two signals which are assigned to CO vibrations are observed at 2048 and 2096 cm⁻¹. The mass spectra indicate that the iodide ions are coordinated to the iron centre.

UV/Visible-NIR Spectroscopy of the Complexes: The square-planar coordination environment of the nickel centres in all of the complexes is reflected in their ligand field spectra. The data are presented in Table 3. All complexes are brown solids and yield pale brown solutions in both chloroform and acetonitrile. Only small differences are observed between the UV/Visible-NIR spectra of the complexes in chloroform and in acetonitrile, indicating that in all cases solvent coordination does not take place and decomposition in solution is not within the timescale of the experiment.

Table 3. Electronic absorption maxima for the Ni^{II} complexes 1–4

	$\tilde{\nu}/\text{cm}^{-1}$ ($\epsilon/\text{mol}^{-1}\cdot\text{L}\cdot\text{cm}^{-1}$)		
	Solid state	Chloroform	Acetonitrile
[Ni(xbsms)FeCl ₂] ₂ (1)	16 600		
	19 200	19 200 (1017)	20 000 (1547)
	23 700	23 900 (2221)	23 500 (3535)
	30 200		31 000 (7843)
[Ni(xbsms)Fe(CO) ₄] (2)		34 900 (16135)	33 900 (9074)
	14 400	15 000 (530)	15 000 (330)
	19 500	20 800 (2612)	
	23 900	25 300 (5241)	25 900 (3943)
	29 800	31 000 (6460)	30 600 (8167)
[Ni(xbsms)Fe(NO) ₂] (3)	36 700		35 500 (14142)
	13 600		19 900 (sh)
	24 800	25 900 (sh)	25 000 (sh)
		30 200 (sh)	30 600 (6400)
[Ni(xbsms)Fe(CO) ₂ I ₂] (4)		34 900 (16200)	34 900 (13800)
	10 800		
	14 300		
	19 300		20 000 (sh)
	23 400	22 500 (sh)	23 900 (4392)
		27 000 (4668)	27 900 (7719)
	34 900	34 400 (3108)	35 000 (36409)

The d–d transitions involving the nickel centre in the complex [Ni(xbsms)FeCl₂]₂ are at a higher energy than those in the complex [Ni(xbsms)], and the LMCT transitions are at a lower energy.^[20] This can be explained by the fact that the iron centre in complex 1 has electron-donating chloride ions, and this results in a higher electron-density on the thiolate sulfur atoms. These thiolate sulfur atoms then donate more electron-density to the nickel centre, and as a result the nickel–thiolate distance is shorter. This observation is in agreement with the crystal structure. The shortening of this nickel–thiolate bond leads to longer thioether sulfur–nickel distances.

For 2 and 3, the shift in energy is the opposite. As a result of the π back-donation from the iron centre to the CO ligands in 2 and NO ligands in 3, the iron centre can accept electron-density from the thiolate sulfur atoms. Hence a lower ligand field splitting occurs, and the d–d absorption maxima are observed at lower energies relative to the parent nickel complex. The absorptions around 35 000 cm⁻¹ in 2 can be explained by a d–d transition involving the iron centre.^[25]

For 4, which has electron-donating iodide ions and electron-withdrawing carbonyl molecules coordinated to the iron centre, both effects are observed. The d–d transitions are at a lower energy relative to [Ni(xbsms)], as is the case for 2; however, the LMCT absorption maxima are also at a lower energy, as is the case for 1. The latter observation also confirms the proposed structure with coordinated iodide ions.

Electrochemical Results: The electrochemical behaviour of the synthesised nickel–iron complexes was investigated using cyclic voltammetry. For complexes 1, 2 and 3 only quasi-reversible and irreversible redox couples were found, which cannot be interpreted unequivocally.

For complex 4, the relevant data are presented in Table 4 and the cyclic voltammogram is shown in Figure 4. For comparison, the cyclic voltammograms of FeI₂ and NEt₄I have been recorded. In MeCN, with NBu₄PF₆ as the supporting electrolyte, FeI₂ shows two reversible waves at 232 mV ($\Delta E = 220$ mV) and 654 mV ($\Delta E = 78$ mV), and NEt₄I shows two reversible waves at 238 mV ($\Delta E = 191$ mV) and 646 mV ($\Delta E = 92$ mV). This indicates that the redox couples at around 250 and 640 mV most likely result from the iodide ions. The couple at around 250 mV appears to arise from a two-electron process, which might result from the oxidation of the iodide ions to I₂. The redox couple at 1246 mV could result from oxidation of the iron centre. Furthermore, 4 shows an irreversible reduction wave at around –500 mV.

The redox behaviour of 4 was also tested in dichloromethane. These data are included in Table 4. In CH₂Cl₂, the oxidation wave at 1206 mV is irreversible. The difference in the redox behaviour in both solvents is significant and probably due to the difference in solubility and ionisation of the complex, and of I⁻ and I₃⁻.

Conclusions and Outlook

Four new nickel–iron complexes have been synthesised from the reactions of the nickel complex [Ni(xbsms)] with FeCl₂, [Fe₂(CO)₉], [Fe(CO)₂(NO)₂] and [Fe(CO)₄I₂].

The [NiFe] complexes with the ligand xbsms are generally less stable than other complexes with the ligands xbsms and bme-daco.^[11,26] This might be as a result of the S₄ coordination environment around the nickel centre, instead of an S₂N₂ coordination environment. Furthermore, most of the [NiFe] complexes show quasi-reversible or irreversible oxidation waves when studied by cyclic voltammetry.

The synthesised compounds appear to be promising complexes for new structural models for the [NiFe]-hydro-

Table 4. Electrochemical data for complexes **4**, compared with [Ni(xbsms)]

[a]	E_{pc} (mV)	E_{pa} (mV)	$E_{1/2}$ (mV)	ΔE (mV)	i_{pa}/i_{pc}
[Ni(xbsms)] (CH ₃ CN) ^[b]	-1572 -508	508 1406			
[Ni(xbsms)Fe(CO) ₂ I ₂] (CH ₃ CN)	-469 (G) 195 (F) 605 (E) 1182 (D)	308 (A) 679 (B) 1309 (C)	252 642 1246	113 74 127	0.7 0.9 0.6
[Ni(xbsms)Fe(CO) ₂ I ₂] (CH ₂ Cl ₂)	-59 513	352 645 1191	206 579	411 132	1.0 1.0

[a] 1 mM solutions containing 0.1 M NBu₄PF₆ at a scan rate of 0.2 V/s; Pt working electrode, Pt auxiliary electrode and an Ag/AgCl reference electrode. $E_{1/2}$ in mV vs. Ag/AgCl. The letter at the E value corresponds to the oxidative or reductive wave of the cyclic voltammogram, shown in Figure 4. [b] Taken from ref.^[20]

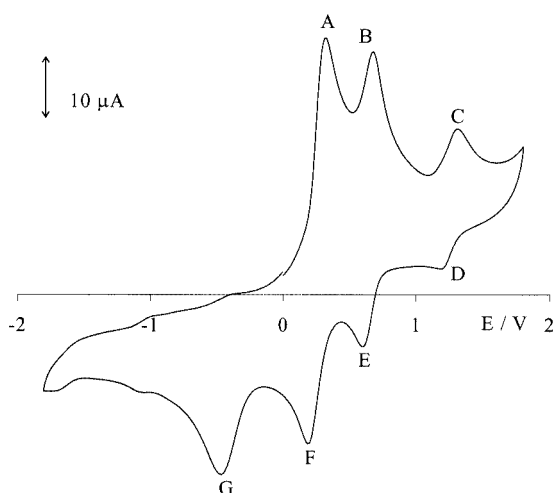


Figure 4. Cyclic voltammogram of [Ni(xbsms)Fe(CO)₂I₂] (**4**) at a scan rate of 0.2 V/s (1 mM solution in acetonitrile containing 0.1 M Bu₄NPF₆). E vs. Ag/AgCl

genases. An improved model for the hydrogenase active site may be achieved by exchanging the iodide ions in complex **4** for cyanide molecules, and this work is in progress.

In the near future, the complexes will be screened for hydrogenase activity by means of reaction with dihydrogen or protons.

Experimental Section

Chemicals: All preparations were carried out with reagent grade solvents. All chemicals used in the syntheses were obtained from Acros or Aldrich and were used without further purification, unless otherwise mentioned. The complexes were synthesised under argon using standard Schlenk techniques. Solvents were deoxygenated by bubbling a stream of argon through the solution, or by the freeze-pump-thaw method, and were dried with molecular sieves. The complexes [Ni(xbsms)],^[20] [Fe(CO)₂(NO)₂]^[27] and [Fe(CO)₄I₂]^[28] were synthesised according to published methods.

Physical Measurements: The IR spectra were recorded with a Perkin–Elmer FT-IR Paragon 1000 spectrophotometer equipped with a golden gate ATR device, using the reflectance technique (4000–300 cm⁻¹, resolution 4 cm⁻¹). Elemental analyses were carried out with a Perkin–Elmer series II CHNS/O analyzer 2400. Metal analyses were performed with a Perkin–Elmer 3100 atomic absorption (AAS) and flame emission spectrometer using a linear calibration method. Ligand field spectra were recorded with a Perkin–Elmer Lambda 900 spectrophotometer. The diffuse reflectance technique, with MgO as a reference, was used for the solid compounds. Ligand field spectra of the solutions were obtained with the used solvent in the reference beam. NMR spectra were recorded with a Bruker WM 300 MHz spectrometer or on a Bruker AV 400 MHz spectrometer. Proton and carbon chemical shifts are indicated in ppm relative to tetramethylsilane (TMS). The electrochemical measurements were performed with an Autolab PGstat10 potentiostat controlled by GPES4 software. A three-electrode system was used, consisting of a platinum working electrode, a platinum auxiliary electrode and an Ag/AgCl reference electrode. The experiments were carried at room temperature under argon with tetrabutylammonium hexafluorophosphate (0.10 M) as the electrolyte. Under these conditions the ferrocenium-ferrocene couple is at +430 mV, with a peak separation of 59 mV. All potentials are reported relative to Ag/AgCl. Mass analyses were performed with a Finnigan MAT 900 equipped with an Electrospray interface (ESI). Spectra were collected by constant infusion of the sample dissolved in methanol/water containing 1% HOAc. Room temperature magnetic susceptibility measurements were performed using a magnetic susceptibility balance type MK1 or using the NMR method.^[29]

[Ni(xbsms)FeCl₂]₂ (1): FeCl₂·4H₂O (0.049 g, 0.25 mmol) was added to a solution of [Ni(xbsms)] (0.100 g, 0.25 mmol) in acetonitrile (20 mL). After stirring for 2 h, the precipitate formed was collected by filtration. A brown product was obtained, with a yield of 0.082 g (62%). Single crystals suitable for X-ray diffraction were obtained from the filtrate on standing. IR: $\tilde{\nu}_{max}$ = 2975 w, 2947 w, 1486 w, 1440 m, 1380 m, 1362 m, 1300 w, 1256 m, 1223 m, 1192 m, 1135 s, 1075 s, 1007 w, 952 m, 890 m, 865 w, 772 s, 756 w, 730 m, 684 s, 608 s, 580 m, 544 m, 469 m, 418 w, 373 w, 310 s cm⁻¹. C₃₂H₄₈Cl₄Fe₂Ni₂S₈ (1060.1): calcd. C 36.25, H 4.56, S 24.19, Ni 11.08, Fe 10.54; found C 36.47, H 4.61, S 22.87, Ni 11.17, Fe 10.21.

[Ni(xbsms)Fe(CO)₄] (2): [Fe₂(CO)₉], (0.090 g, 0.25 mmol) was added to a solution of [Ni(xbsms)] (0.20 g, 0.50 mmol) in acetonitrile

(30 mL). After stirring for 3 h, [Fe₂(CO)₉] had completely dissolved. The acetonitrile was partly evaporated in vacuo until a precipitate was formed. The precipitate was collected by filtration, giving a brown product with a yield of 0.11 g (41%). ¹H NMR [300.13 MHz, CD₃CN, 298 K, see Figure 2 for numbering scheme]: δ = 7.52 (m, 1 H, C⁵-H), 7.46 (m, 1 H, C¹¹-H), 7.38 (m, 2 H, C⁶-H, C¹²-H), 4.76 (d, ²J_{H,H} = 10.9 Hz, 1 H, C³HH), 4.38 (d, ²J_{H,H} = 10.9 Hz, 1 H, C³HH), 4.01 (d, ²J_{H,H} = 11.6 Hz, 1 H, C⁹HH), 3.91 (d, ²J_{H,H} = 11.6 Hz, 1 H, C⁹HH), 3.05 (d, ²J_{H,H} = 13.0 Hz, 1 H, C¹HH), 2.97 (d, ²J_{H,H} = 13.0 Hz, 1 H, C¹HH), 2.81 (d, ²J_{H,H} = 12.3 Hz, 1 H, C⁷HH), 2.46 (d, ²J_{H,H} = 12.3 Hz, 1 H, C⁷HH), 1.82 (s, 3 H, C²-Me), 1.71 (s, 3 H, C⁸-Me), 1.60 (s, 3 H, C⁸-Me), 1.43 (s, 3 H, C²-Me) ppm. ¹³C APT NMR [100.62 MHz, [D₆]acetone, 253 K]: δ = 135.37 (C¹⁰), 134.20 (C⁴), 133.41 (C⁵), 131.63 (C¹¹), 129.38 (C⁶), 129.11 (C¹²), 67.19 (C²), 62.41 (C⁸), 48.01 (C³), 40.63 (C⁹), 35.29 (C¹), 34.92 (C⁷), 27.04 (C²-CH₃), 26.43 (C²-CH₃), 25.20 (C⁸-CH₃), 25.13 (C⁸-CH₃) ppm. IR: ν_{max} = 2930 w, 2922 w, 2830 w, 2009 vs, 1944 vs, 1861 vs, 1456 m, 1435 m, 1380 m, 1260 m, 1234 w, 1212 w, 1188 w, 1165 w, 1133 m, 1070 m, 1002 w, 948 w, 892 m, 871 w, 781 s, 759 m, 706 m, 684 w, 616 s, 595 s, 571 s, 559 s, 490 m, 468 m, 436 m, 398 m, 368 s, 340 m cm⁻¹. C₂₀H₂₄FeNiO₄S₄ (571.2): calcd. C 42.06, H 4.23, S 22.45, Ni 10.28, Fe 9.78; found C 41.67, H 4.78, S 22.07, Ni 10.59, Fe 9.29. ESI-MS: m/z = 543 [M - "CO" + H]⁺.

[Ni(xbsms)Fe(NO)₂] (3): A solution of [Fe(CO)₂(NO)₂] (0.058 g, 0.34 mmol) in acetonitrile (3 mL) was added to a solution of [Ni(xbsms)] (0.137 g, 0.34 mmol) in acetonitrile (40 mL) at 273 K. Whilst stirring for 2 h, the evolution of a gas was observed, indicating the loss of CO. After the reaction was completed, the acetonitrile was partly evaporated until a precipitate was formed. This precipitate was collected by filtration to give a brown solid with a yield of 0.71 g (55%). ¹H NMR [300.13 MHz, CDCl₃, 300 K]: δ = 7.25 (m, 4 H, Ph-H), 3.98 (s, 4 H, Ph-CH₂-S-), 3.20 (s, 4 H, -(C(CH₃)-CH-S-), 1.61 (s, 12 H, CH₃) ppm. IR: ν_{max} = 2934 w, 2928 w, 1809 w, 1771 s, 1733 vs, 1700 m, 1456 m, 1381 m, 1360 m, 1228 w, 1136 m, 1118 m, 1085 m, 957 m, 886 w, 786 m, 702 m, 554 w, 492 w, 469 m, 350 w, 302 m cm⁻¹. C₁₆H₂₄FeN₂NiO₂S₄·0.5 CH₃CN (539.8): calcd. C 37.83, H 4.76, N 6.49, S 23.76, Ni 10.81, Fe 10.35; found C 38.22, H 5.48, N 6.06, S 21.43, Ni 10.96, Fe 10.21.

[Ni(xbsms)Fe(CO)₂I₂] (4): [Fe(CO)₄I₂] (0.105 g, 0.25 mmol) was added to a solution of [Ni(xbsms)] (0.101 g, 0.25 mmol) in chloroform (12 mL) at 273 K. After stirring for 1.5 h in the absence of light, the precipitate was collected by filtration. A brown product was obtained, with a yield of 0.050 g (24%). IR: ν_{max} = 2959 m, 2948 m, 2096s, 2048s, 1456s, 1417 m, 1389 m, 1372s, 1225 m, 1136s, 1081s, 955 m, 882 m, 772 vs, 694s, 606s, 570 m, 492s, 468s, 350s, 310m cm⁻¹. C₁₈H₂₄FeI₂NiO₂S₄ (769.0): calcd. C 28.11, H 3.15, S 16.68, Ni 7.64, Fe 7.26; found C 27.63, H 3.38, S 16.18, Ni 7.85, Fe 6.86. ESI-MS: m/z = 644 [Ni(xbsms)Fe(CO)₂I]⁺, 616 [Ni(xbsms)Fe(CO)I]⁺, 257 [Ni(xbsms)Fe(CO)₂]²⁺, 243 [Ni(xbsms)Fe(CO)]²⁺, 229 [Ni(xbsms)Fe]²⁺.

Crystal Structure Determination of [Ni(xbsms)FeCl₂]₂: X-ray intensities were measured with a Nonius KappaCCD diffractometer with rotating anode (λ = 0.71073 Å) at a temperature of 150 K. The structure was solved with automated Patterson methods (DIRDIF97^[30]) and refined with SHELXL-97^[31] against F² for all reflections. Molecular illustration, structure checking and calculations were performed with the PLATON package.^[32] The crystals

were obtained as dark purple plates. The absorption correction was based on multiple measured reflections (program PLATON^[32] routine MULABS, 0.79–0.89 transmission). Non-hydrogen atoms were refined freely with anisotropic displacement parameters. Hydrogen atoms were located in the difference Fourier map and refined freely with isotropic displacement parameters (methyl groups) or as rigid groups (all other H atoms). Further crystallographic details are given in Table 1.

CCDC-212533 contains the supplementary crystallographic data for this paper. These data can be obtained free of charge at www.ccdc.cam.ac.uk/conts/retrieving.html [or from the Cambridge Crystallographic Data Centre, 12, Union Road, Cambridge CB2 1EZ, UK; Fax: (internat.) +44-1223/336-033; E-mail: deposit@ccdc.cam.ac.uk].

Acknowledgments

Prof. Dr. Jan Reedijk is gratefully acknowledged for fruitful discussions. This work was supported in part (M.L., A.L.S.) by the Council for Chemical Sciences of the Netherlands Organization for Scientific Research (CW-NWO).

- [1] M. W. W. Adams, E. I. Stiefel, *Science* **1998**, *282*, 1842–1843.
- [2] A. C. Marr, D. J. E. Spencer, M. Schröder, *Coord. Chem. Rev.* **2001**, *219*, 1055–1074.
- [3] J. Alper, *Science* **2003**, *299*, 1686–1687.
- [4] R. K. Thauer, A. R. Klein, G. C. Hartmann, *Chem. Rev.* **1996**, *96*, 3031–3042.
- [5] A. Volbeda, E. Garcia, C. Piras, A. L. de Lacey, V. M. Fernandez, E. C. Hatchikian, M. Frey, J. C. Fontecilla-Camps, *J. Am. Chem. Soc.* **1996**, *118*, 12989–12996.
- [6] Y. Higuchi, T. Yagi, N. Yasuoka, *Structure* **1997**, *5*, 1671–1680.
- [7] E. Bouwman, R. K. Henderson, A. L. Spek, J. Reedijk, *Eur. J. Inorg. Chem.* **1999**, 217.
- [8] R. K. Henderson, E. Bouwman, A. L. Spek, J. Reedijk, *Inorg. Chem.* **1997**, *36*, 4616.
- [9] V. E. Kaasjager, J. van den Broeke, R. K. Henderson, W. J. J. Smeets, A. L. Spek, W. L. Driessen, E. Bouwman, J. Reedijk, *Inorg. Chim. Acta* **2001**, *316*, 99–104.
- [10] G. Musie, J. H. Reibenspies, M. Y. Darensbourg, *Inorg. Chem.* **1998**, *37*, 302–310.
- [11] D. K. Mills, Y. M. Hsiao, P. J. Farmer, E. V. Atnip, J. H. Reibenspies, M. Y. Darensbourg, *J. Am. Chem. Soc.* **1991**, *113*, 1421–1423.
- [12] V. E. Kaasjager, E. Bouwman, S. Gorter, J. Reedijk, C. A. Grapperhaus, J. H. Reibenspies, J. J. Smee, M. Y. Darensbourg, A. Derecskei-Kovacs, L. M. Thomson, *Inorg. Chem.* **2002**, *41*, 1837–1844.
- [13] M. A. Halcrow, G. Christou, *Chem. Rev.* **1994**, *94*, 2421–2481.
- [14] M. C. Smith, J. E. Barclay, S. P. Cramer, S. C. Davies, G. Wei-Wei, D. L. Hughes, S. Longhurst, D. J. Evans, *J. Chem. Soc., Dalton Trans.* **2002**, 2641–2647.
- [15] F. Osterloh, W. Saak, D. Haase, S. Pohl, *Chem. Commun.* **1997**, 979–980.
- [16] C. H. Lai, J. H. Reibenspies, M. Y. Darensbourg, *Angew. Chem. Int. Ed. Engl.* **1996**, *35*, 2390–2393.
- [17] W. F. Liaw, C. Y. Chiang, G. H. Lee, S. M. Peng, C. H. Lai, M. Y. Darensbourg, *Inorganic Chemistry* **2000**, *39*, 480–484.
- [18] M.-C. Chalbot, A. M. Mills, A. L. Spek, G. J. Long, E. Bouwman, *Eur. J. Inorg. Chem.* **2003**, 453–457.
- [19] D. Sellmann, F. Geipel, F. Lauderbach, W. Heinemann, *Angew. Chem. Int. Ed.* **2002**, *41*, 632–634.
- [20] J. A. W. Verhagen, D. D. Ellis, M. Lutz, A. L. Spek, E. Bouwman, *J. Chem. Soc., Dalton Trans.* **2002**, 1275–1280.

- [21] A. W. Addison, R. T. Nageswara, J. Reedijk, J. v. Rijn, G. C. Verschoor, *J. Chem. Soc., Dalton Trans.* **1984**, 1349.
- [22] A. P. Ginsberg, M. E. Lines, K. D. Karlin, S. J. Lippard, F. J. DiSalvo, *J. Am. Chem. Soc.* **1976**, *98*, 6958.
- [23] A. J. Pierik, W. Roseboom, R. P. Happe, K. A. Bagley, S. P. J. Albracht, *J. Biol. Chem.* **1999**, *274*, 3331–3337.
- [24] K. Nakamoto, *Infrared and raman spectra of inorganic and coordination compounds*, John Wiley & Sons, New York, **1997**, ed. 5, p. 149–150.
- [25] M. Dartiguenave, Y. Dartiguenave, H. B. Gray, *Bull. Soc. Chim. Fr.* **1969**, 4223.
- [26] G. Musie, P. J. Farmer, T. Tuntulani, J. H. Reibenspies, M. Y. Darensbourg, *Inorg. Chem.* **1996**, *35*, 2176–2183.
- [27] W. Hieber, H. Beutner, *Z. Anorg. Allg. Chemie* **1963**, *320*, 101–111.
- [28] W. Hieber, G. Bader, *Ber. Dtsch. Chem. Ges.* **1928**, *61*, 558–563.
- [29] D. F. Evans, *J. Chem. Soc.* **1959**, 2003–2005.
- [30] P. T. Beurskens, G. Admiraal, G. Beurskens, W. P. Bosman, S. Garcia-Granda, R. O. Gould, J. M. M. Smits, C. Smykalla, *The DIRDIF97 program system, Technical Report of the Crystallography Laboratory*, University of Nijmegen, Nijmegen, **1997**.
- [31] G. M. Sheldrick, *SHELXL-97. Program for crystal structure refinement*, University of Göttingen, Göttingen **1997**.
- [32] A. L. Spek, *PLATON. A multipurpose crystallographic tool.*, Utrecht University, Utrecht **2000**.

Received May 14, 2003